Epidemics 8 (2014) 28–40

Contents lists available at ScienceDirect

Epidemics

journal homepage: www.elsevier.com/locate/epidemics

Speed versus coverage trade off in targeted interventions during an outbreak

Axel A. Bonačić Marinović[a,b,*], Marion Koopmans[a], Sabine Dittrich[a,c,d,e], Peter Teunis[a], Corien Swaan[a], Jim van Steenbergen[a,f], Mirjam Kretzschmar[a,b]

[a] Centre for Infectious Disease Control, National Institute for Public Health and the Environment, Bilthoven, The Netherlands
[b] Julius Centre for Health Sciences & Primary Care, University Medical Centre Utrecht, The Netherlands
[c] European Public Health Microbiology Training Program (EPIET/EUPHEM), European Centre for Disease Prevention and Control, Stockholm, Sweden
[d] Lao-Oxford-Mahosot Hospital-Wellcome Trust Research Unit, Microbiology Laboratory, Mahosot Hospital, Vientiane, Lao Democratic People's Republic
[e] Centre for Clinical Vaccinology and Tropical Medicine, Nuffield Department of Medicine, Churchill Hospital, University of Oxford, Oxford, England, UK
[f] Centre for Infectious Diseases, Leiden University Medical Centre, Leiden, The Netherlands

ARTICLE INFO

Article history:
Received 23 September 2013
Received in revised form 1 April 2014
Accepted 14 May 2014
Available online 15 August 2014

Keywords:
Outbreak control
Influenza
Timeliness
Coverage
Sensitivity
Diagnostic

ABSTRACT

Which case-based intervention measures should be applied during an epidemic outbreak depends on how timely they can be applied and how effective they are. During the course of each individual's infection, the earlier control measures are applied on him/her the more effectively further disease spread can be prevented. However, quick implementation can lead to loss of efficacy or coverage, e.g., when individuals are targeted based on rapid but poorly sensitive diagnostic tests in place of slower but accurate PCR tests. To analyse this trade off between speed and coverage we used stochastic models considering how the individual reproduction density is modified by interventions. We took as example the case-based intervention strategy employed in the Netherlands during the beginning of the H1N1 pandemic. Suspected cases were isolated and samples were collected for PCR diagnosis. In case of positive diagnosis, antiviral drugs were provided to contacts as post-exposure prophylaxis. At the time there were also rapid influenza diagnostic tests (RIDTs) available which provided results within an hour after sample collection compared to a median of 2.7 days for PCR tests, but they were less sensitive. We studied how interventions based on RIDTs with various sensitivities affect the outbreak size and how these compare to PCR diagnosis based interventions. Using an intervention based on a bedside RIDT with 60% detection ratio or a laboratory RIDT with 70% detection ratio is as effective as the most effective PCR-diagnosis based intervention. Relative performances of interventions are not dependent on the basic reproduction number R_0 but only on distributions of individual reproduction density and of delay periods. The individual reproduction density combines R_0 and infection time distribution, both crucial in determining the impact of case-based interventions during epidemic outbreaks.

Introduction

Different types of intervention can be applied during epidemic outbreaks in an attempt to reduce outbreak effects, such as final size, incidence, prevalence, morbidity and mortality. Case-based interventions are focused around infected individuals. They are applied at a time which is specific for each individual, depending on when he/she is identified (or suspected) as infected, and reduce the individual's infectious potential from then on. For example, isolation, quarantine, post-exposure prophylaxis of infected and traced contacts would be case-based interventions.

Success of a case-based intervention in reducing the number of subsequent infections is directly linked with how timely it is implemented and how complete the implementation coverage is: the earlier the implementation and the higher its coverage, the more effective the intervention is. But there are situations where a quicker intervention implementation is only possible at the cost of coverage loss and vice versa, e.g., when the intervention is based on a quicker but less sensitive diagnostic test versus a slower but more

* Corresponding author at: Centre for Infectious Disease Control, National Institute for Public Health and the Environment, Bilthoven, The Netherlands.
Tel.: +31 302748654.
E-mail addresses: axel.bonacic.marinovic@rivm.nl, abonacicm@gmail.com (A.A. Bonačić Marinović).

http://dx.doi.org/10.1016/j.epidem.2014.05.003

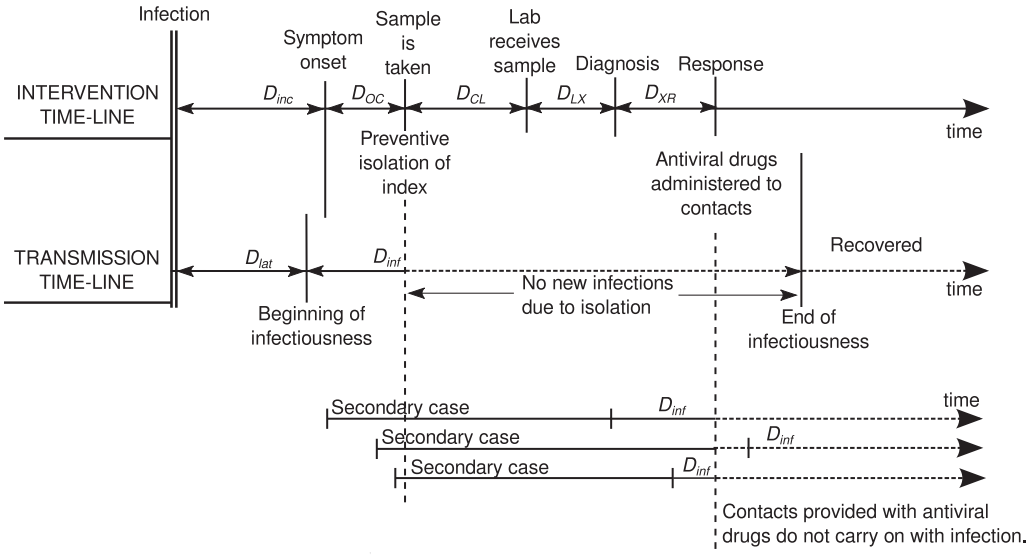

Fig. 1. Schematic time-line of the intervention applied to positively diagnosed individuals and to their high risk contacts from the moment of infection of the index case. Durations of different periods are indicated as D_{lat} for latency (individual infected but not yet infectious), D_{inf} for infectious, D_{inc} for incubation (time to symptom onset), D_{OC} for period between symptom onset and consulting the general practitioner (which coincides with the collection of samples for diagnosis), D_{CL} time for transporting samples to the laboratory, and D_{LX} time between arrival to laboratory and diagnosis result, D_{XR} time to apply response on contacts after a diagnosis is positive.

sensitive diagnosis. Because of this trade-off it is not directly clear which kind of diagnostic test would render a case-based intervention more effective.

We analysed the case-based intervention strategy implemented in the Netherlands during the beginning of the H1N1 pandemic. In combination with providing general hygiene advice when novel influenza A (H1N1) was detected in the Netherlands, a case-based intervention plan was put in place to contain the spreading of the new influenza virus (Hahné et al., 2009). Fig. 1 shows a schematic time-line of the intervention. Suspected cases were isolated while samples were transported to specialised laboratories for diagnosis by polymerase chain reaction (PCR) tests (Meijer et al., 2009; van Asten et al., 2009). High risk contacts of suspected cases were located and in case of a positive diagnosis anti-viral drugs were administered to them as post-exposure prophylaxis (PEP). PCR diagnostics sensitivity is less than ideal given that the viral load content of field collected samples is highly variable and dependent on the infection-age at which it is collected [e.g., van Boven et al., 2010]. But given appropriate influenza viral RNA samples, the typing of novel influenza A (H1N1) based on PCR has a high sensitivity [e.g., Vinikoor et al., 2009, Bouscambert Duchamp et al., 2010]. Therefore, PCR diagnostic tests are considered the gold standard method to evaluate sensitivity of other diagnostic techniques. However, besides the need for specifically dedicated personnel, laboratory and equipment, PCR tests are time consuming: Although one PCR diagnostic test can take up to 8 h in the laboratory (from receiving the sample to reporting the test result), the time between sample collection and reporting the result is considerably extended due to transport, queueing, working schedules and other logistics. At the time there were also commercially available, widely used, rapid influenza diagnostic tests (RIDTs). These tests are portable, have no need of specialised resources or personnel, and provide a result within the hour. RIDTs can be performed at the bedside or as quick tests at laboratory locations [e.g, Crawford et al., 2010]. However, despite their speed and ease of use, RIDTs were discarded as reliable diagnostic tests in the Netherlands because their overall sensitivity to novel influenza A (H1N1) viral antigens was between 40% and 69% when compared to the PCR gold standard technique (Balish et al., 2009; Jernigan et al., 2011).

The question arises whether and when using RIDTs in place of PCR tests for diagnosis of the novel influenza A (H1N1) would have rendered the applied interventions more effective. To answer this question we used stochastic models of H1N1 influenza outbreaks that follow each infector individually, from the moment he/she has been infected. The models include the concept of individual reproduction density, which is the rate of infections produced per unit time by an infector at any given infection-age (the time passed since becoming infected). This provides flexibility to follow the new cases each infector will generate as his/her individual reproduction density can be modified depending on whether and how late after infection an intervention is applied onto him/her. We analysed the results of our models to determine which diagnostic test would have rendered the intervention more effective in reducing the growth of the epidemic, depending on diagnostic test speed and sensitivity.

Methods

We modelled the Dutch situation at the introduction of the novel influenza A (H1N1) in 2009 by assuming implementation of intervention measures based on RIDTs performed at the bedside and based on RIDTs performed at laboratory locations with varying sensitivities. We compared these results to those from models assuming implementation of intervention measures based on the standard PCR diagnosis. To evaluate the performance of the different interventions we focused on the attack rate: the lower it is the better the performance of the intervention is.

Individual reproduction density and interventions

The basic reproduction number, R_0, indicates the average number of new infectees that a random infector produces during his infectious period in a completely susceptible population, in the absence of any intervention. If $R_0 < 1$ an outbreak will die out without becoming large, but if $R_0 > 1$ it is likely that the outbreak becomes large, i.e., affects a significant fraction of the population. The individual reproduction number corresponds to the expected number of new infectees that a particular infector produces during his infectious period (Lloyd-Smith et al., 2005). We write the individual reproduction number of a particular infector as R_j. We denote with a subscript j all quantities corresponding to a particular subject j, meaning that these quantities tend to vary among

Table 1
Model parameter values.

Parameter	Notation	Value/distribution	Reference
Duration of incubation period (distribution)	D_{inc}	*logNormal*(1.047, 0.642); 1–7days, with mean 3 days and SD 2.5 days	RIVM (2010), Heymann (2008), Richardson et al. (2001)
Duration of latent period (distribution)	D_{lat}	$D_{\text{inc}} - logNormal(-1.040, 0.833)$; infectiousness starts between 1 and 0 days before onset of symptoms	RIVM (2010), Heymann (2008), Richardson et al. (2001)
Duration of infectious period (distribution)	D_{inf}	$(D_{\text{inc}} - D_{\text{lat}} + logNormal(2.013, 0.067)$; infectious period ends about 7 days after symptom onset	RIVM (2010), Heymann (2008), Richardson et al. (2001)
Time elapsed between symptom onset and sample collection for diagnosis (distribution)	D_{OC}	*logNormal*(0.996, 0.813); mean 3.77 days and SD 3.65 days	Fit to data gathered by IDS
Time elapsed between sample collection and arrival to laboratory (distribution)	D_{CL}	*logNormal*(0.335, 0.331); mean 1.48 days and SD 0.50 days	Fit to data gathered by IDS
Time elapsed between arrival to laboratory and diagnosis result (distribution)	D_{LX}	*logNormal*(0.050, 0.954); mean 1.66 days and SD 0.954 days	Fit to data gathered by IDS
Time elapsed between diagnosis result and PHA response on contacts	D_{XR}	Fixed value 0.75 days	Approximation to LCI expert opinion
Shape of viral load curve as function of infection-age	$f_{\text{VL}}(\tau)$	$logNormalPDF(\tau - D_{\text{lat}}; 1.03, 0.67)$, log-normal probability density distribution, evaluated at age since onset of infectiousness $(\tau - D_{\text{lat}})$	Dolin (1976), Carrat et al. (2008), Cori et al. (2012)

different individuals. The average value of R_j in a completely susceptible population in the absence of intervention corresponds to R_0. Reproduction numbers describe the cumulative number of infections produced during the whole infectious period by an infector, but the rate at which he infects new individuals is not necessarily constant. It depends on the infectivity and contacts the infector has during his infectious period, both depending on the infection-age. In analogy with the notation in Diekmann et al. (2012), consider τ_j the infection-age of infector j, $A_j(\tau_j)$ his infectivity and $c_j(\tau_j)$ the rate he makes contact with others after he had become infected. We define the individual reproduction density $\varrho_j(\tau_j) \equiv c_j(\tau_j)A_j(\tau_j)$, the rate at which a particular infector j produces new infectees at a given infection-age τ_j. The individual reproduction number can be written as

$$\int_0^\infty \varrho_j(\tau_j)d\tau_j = R_j. \tag{1}$$

After applied at infection-age $\tau_{\mathcal{I},j}$ on infector j, an individual-based intervention $\mathcal{I}$ lowers $\varrho_j(\tau_j)$ values, depending on how effective it is. Thus, we consider the individual reproduction number modified by the intervention as

$$R_{\mathcal{I},j} = \int_0^{\tau_{\mathcal{I},j}} \varrho_j(\tau_j)d\tau_j + \int_{\tau_{\mathcal{I},j}}^\infty (1 - \mathcal{I}_{\text{eff}})\varrho_j(\tau_j)d\tau_j, \tag{2}$$

where intervention effectiveness $\mathcal{I}_{\text{eff}}$ ranges from 0 to 1, with 1 meaning 100% effective. An intervention would successfully stop an epidemic outbreak if the mean reproduction number modified by the intervention $\overline{R_{\mathcal{I},j}} \equiv R_{\mathcal{I}} < 1$.

Stochastic model of Dutch response to novel influenza A (H1N1)

The aim of this study is to asses which intervention would be more effective in reducing the number of infected people during an outbreak without putting attention on health economics. Therefore, we assume that the studied interventions do not carry implementation, logistics and/or economic burden, and neglect problems regarding treating non-infected contacts. We use a stochastic model similar to that of Bonačić Marinović et al. (2012), which does not track susceptible individuals, by employing a combined compartmental and individual approach. Persons not yet infected (the susceptibles) are considered in one compartment where they cannot be distinguished from each other. At infection, the infected individual moves out of the susceptible compartment and is then followed individually throughout his disease history in time steps of 6 h. We record the individual reproduction density of each infector as it becomes modified depending on the infection-age at which interventions are applied.

Individual time-lines

Every individual who has been infected has two internal time-lines that characterise the development and consequences of the disease according to his infection-age (Fig. 1). The transmission time-line tracks the duration of the different infectious states of the individual. It starts with a latent period of duration D_{lat}, then the individual becomes an infector and remains infectious for a period of duration D_{inf}, until he is no longer infectious because he recovers permanently (see Table 1 for period distributions). The intervention time-line tracks the different stages of the disease, which can be observed and which finally lead to an individually targeted intervention. It begins with an incubation period of duration D_{inc} until onset of symptoms. Then there is a time interval of duration D_{OC} from onset of symptoms until consultation with a physician or local public health authority (PHA), at which time samples for diagnosis are collected. For performing PCR diagnosis, samples need to be transported to the laboratory and this period lasts D_{CL}. Once in the laboratory, a time period of duration D_{LX} is needed to obtain the PCR diagnostic test results. If a sample is tested positive, a period of duration D_{XR} is needed by local PHAs to effectuate the intervention on high risk contacts.

Probability distribution of various time-line periods

Period duration values for both time-lines are generated randomly from the distributions indicated in Table 1 for each infected individual. Distributions for the periods D_{inc}, D_{lat} and D_{inf} were constructed based on published literature. Distributions of D_{OC}, D_{CL} and D_{LX} were constructed using data collected by the Centre for Infectious Disease Research, Diagnostics and Screening (IDS) of the Dutch National Institute for Public Health and the Environment (RIVM), the reference laboratory in charge of pandemic influenza diagnostics during the early phase of the outbreak in the Netherlands. Parameters of the distributions in Table 1 were found by fitting the data with a Kolmogorov-Smirnov minimisation at a 0.05 significance level. We assumed a fixed delay D_{XR} of 18 h for PHAs to respond with administration of PEP to high risk contacts, based on expert opinion from the Dutch National Coordination Centre for Communicable Disease Control (LCI).

Viral load shaping individual reproduction density

We assumed that in our simulated population of 10,000 individuals everyone has the same probability of contacting everyone else, so-called homogeneous mixing. Any given infector, say j, has a probability per time step $P_{\mathrm{inf},j}(\tau_j)d\tau_j$ of infecting a susceptible, dependent on the infection-age τ_j and proportional to the individual reproduction density $\varrho_j(\tau_j)$. We consider the viral load curve shape $f_{\mathrm{VL},j}(\tau_j)$, which peaks one and a half days after the onset of symptoms (Table 1) as for seasonal influenza (Dolin, 1976; Carrat et al., 2008; Cori et al., 2012). Note that $f_{\mathrm{VL},j}(\tau_j)$ does not represent the actual viral load values in time, but only its scaled shape as a function of the infection-age. In case that subject j moves freely during his whole infectious period we assume $\varrho_j(\tau_j)$ proportional to his viral load during the infectious period only. This implies

$$P_{\mathrm{inf},j}(\tau_j) \propto \begin{cases} f_{\mathrm{VL},j}(\tau_j) & \text{if } D_{\mathrm{lat}} < \tau_j < (D_{\mathrm{lat}} + D_{\mathrm{inf}}) \\ 0 & \text{otherwise} \end{cases}. \quad (3)$$

For each assumed R_0 value in our simulations, the amplitude of $P_{\mathrm{inf},j}(\tau_j)$ was chosen such that outbreak final sizes from our simulations assuming no intervention on contacts is applied were consistent with the final-size equation $\ln(s_\infty) = R_0(s_\infty - 1)$, where s_∞ is the final size [e.g., Anderson and May, 1991, Diekmann et al., 2012].

Isolation of newly suspected cases

As part of the response plan in the Netherlands to control the novel influenza pandemic in 2009, suspected cases (not their contacts) were instructed to remain isolated. We assumed that after samples for diagnosis are collected, infected individuals cannot infect any others due to 100% effective isolation. This reduces $\varrho_j(\tau_j)$ to zero when $\tau_j > D_{\mathrm{inc},j} + D_{\mathrm{OC},j}$ in all cases (Fig. 2).

Intervention on contacts of positive cases: post-exposure prophylaxis

In addition to the isolation of suspected cases, high risk contacts of positively diagnosed cases were provided antiviral drugs to prevent disease and further transmission (PEP). In our models this means that at the moment a case is diagnosed, those infected directly by him receive PEP treatment and have a reduced reproduction density from then on (Fig. 2). The effectiveness of PEP treatment determines the proportion to which the reproduction density is reduced (0 if PEP is 100% effective). Treatment has an effect only if the infected contact receiving it has not yet been isolated.

In the scenario where PCR diagnostic tests are used, infected contacts are treated $D_{\mathrm{CL}}+D_{\mathrm{LX}}+D_{\mathrm{XR}}$ days after samples from the index are collected. In the scenario where bedside RIDTs are used, diagnosis takes place when samples are collected, so infected contacts are treated 18 h (D_{XR}) after sample collection. In the scenario where laboratory RIDTs are used, infected contacts are treated $D_{\mathrm{CL}}+D_{\mathrm{XR}}$ days after collection of samples.

Comparison of scenarios

For comparing the performance of various interventions we used the attack rates. An intervention which shows a lower attack rate was considered to perform better. We compared the attack rate of the epidemic when the intervention uses PCR test diagnosis to that of when bedside RIDTs are used, the latter with a detection ratio in the range of 0–100% when compared to that of the PCR test diagnosis. A similar comparison was carried out between interventions based on PCR test diagnosis and laboratory RIDTs. Comparisons were performed at the end of simulated outbreaks (final attack rate) as this is a direct outcome measure from which the mean reproduction number $R_{\mathcal{I}}$ can be derived. However,

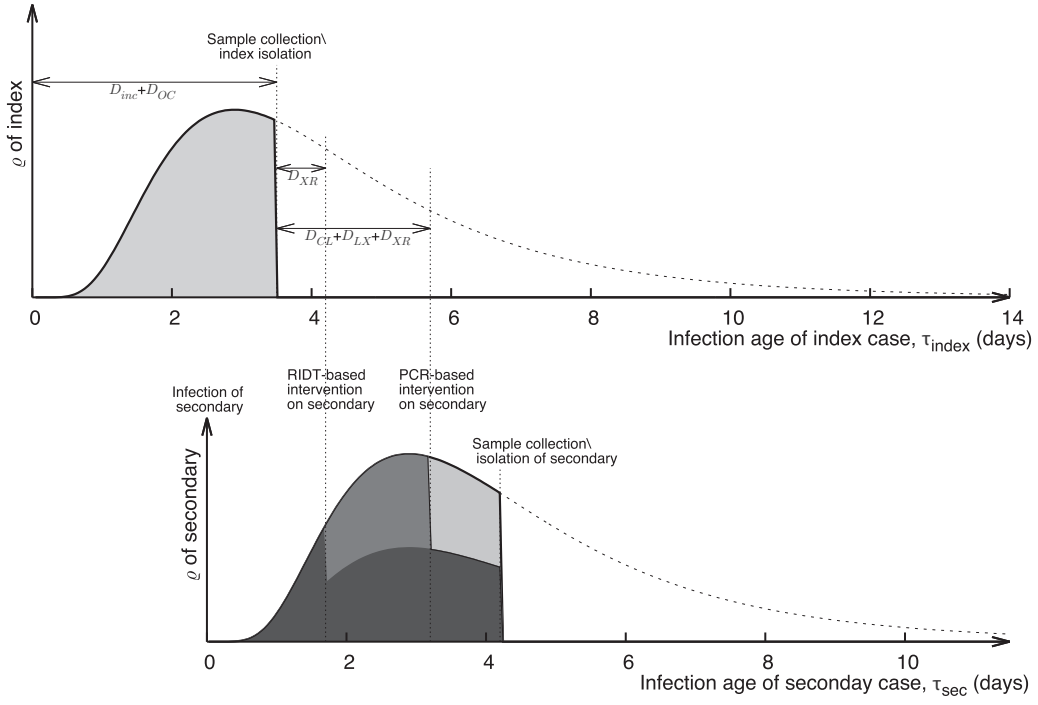

Fig. 2. Schematic time-line of the intervention applied to a positively diagnosed index and to a secondary case in the context of individual reproduction density. Dotted curves represent reproduction densities assuming that neither PEP nor isolation are applied on either the index or the secondary case. Light-grey areas for both cases represent the corresponding individual reproduction number R_{j} affected only by isolation at sample collection due to suspicion of infection, as if cases were independent (secondary case's light-grey area overlaps with darker grey areas). Secondary cases would produce less new cases if antiviral drugs are administered (darker-grey areas) before independent isolation, leading to smaller individual reproduction numbers, $R_{\mathcal{I},j}$. It is assumed for this scheme that PEP is 50% effective, independent of the time that it is administered. The medium-grey area (which overlaps with the darkest-grey area) represents the secondary case's individual reproduction number considering PEP administered at index infection-age $\tau_{\mathcal{I},\mathrm{index}} = D_{\mathrm{inc}} + D_{\mathrm{OC}} + D_{\mathrm{CL}} + D_{\mathrm{LX}} + D_{\mathrm{XR}}$, due to PCR-based diagnosis of index. The darkest-grey area represents the secondary case's smaller individual reproduction number considering PEP administered after positive bedside RIDT results at index infection-age $\tau_{\mathcal{I},\mathrm{index}} = D_{\mathrm{inc}} + D_{\mathrm{OC}} + D_{\mathrm{XR}}$.

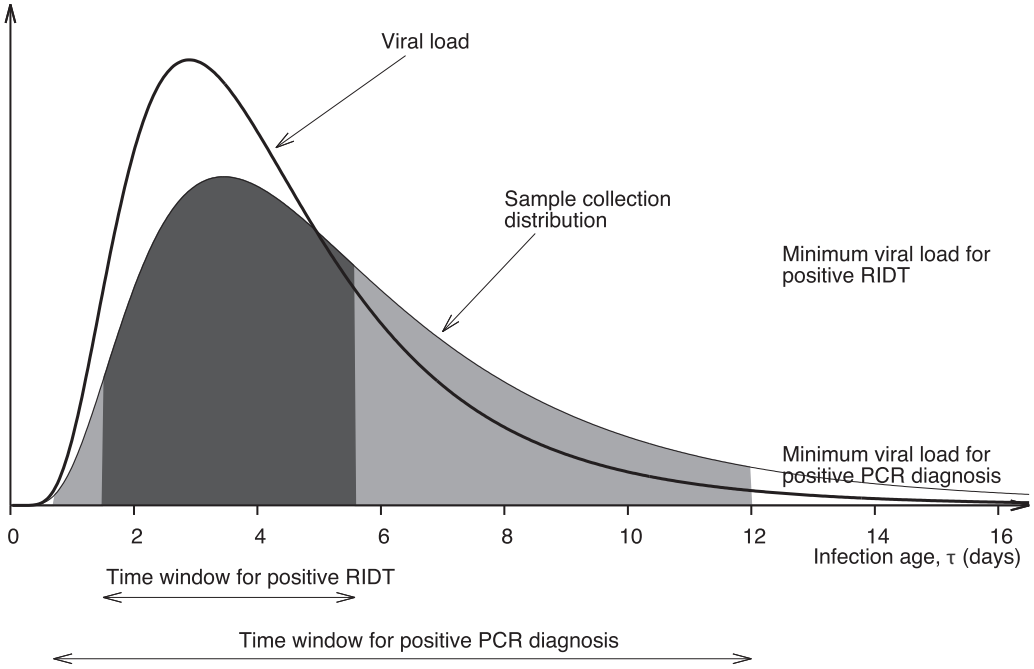

Fig. 3. Viral load since infection and relation to diagnosis test sensitivity. The thick solid line represents the viral load from the moment of infection. Horizontal dotted-lines indicate hypothetical limits for the indicated diagnosis tests to result positive. Vertical dotted-lines indicate time windows within which the indicated tests result positive. The curve with grey area shows the fitted distribution of time elapsed since infection to sample collection (Section "Probability distribution of various time-line periods" and Table 1). The complete greyed area (light- and dark-grey) indicates the proportion of individuals which would be found positive with PCR diagnosis. The dark-grey area indicates the proportion of tested individuals which would be found positive with a RIDT.

case-based interventions are likely to be applied during early stages of an epidemic only and it is of interest for PHAs whether interventions can also slow down the growth of an epidemic as this can buy some time during the outbreak until better control options are developed (e.g., new vaccines). Therefore, for the case of bedside RIDTs we also explicitly performed attack rate comparisons at 30, 60, 90, 120 and 180 days after onset of the epidemic (shown in Appendix A). Some outbreaks die out before the time of observation, in which case their final attack rate is considered.

PCR tests are the gold standard diagnostics method and, although they are not ideal (e.g., field sensitivity of 47% or lower van Boven et al., 2010), for the sake of simplicity we assumed in our models that they are capable of detecting 100% of tested infected cases. This does not affect our results regarding to which intervention would perform better than another because RIDT sensitivities are measured relative to the PCR method. Therefore, the coverage of both RIDT and PCR based interventions would be reduced in the same proportion. Nevertheless, we also considered a scenario where interventions are applied to 50% of the population, included in Appendix B, which is comparable to, e.g., a scenario with 100% coverage intervention and "absolute" sensitivity of PCR test diagnosis of 50%.

We performed our calculations assuming various R_0 values. In our models R_0 is the reproduction number corresponding to a scenario where no PEP intervention on contacts is applied, but only isolation of cases after consultation with a physician or local PHA. To show the effect on the reproduction number caused by the PEP interventions on contacts we derived $R_{\mathcal{I}}$ using our final size results and the final size equation $R_{\mathcal{I}} = (\ln(s_\infty)/(s_\infty - 1))$ [e.g., Anderson and May, 1991, Diekmann et al., 2012].

Following recommendations in international guidelines it is considered that PEP treatment is only effective if administered within 48 h of exposure [e.g., CDC, 2009]. Therefore, we considered scenarios with early (within 48 h of exposure) and late (after 48 h of exposure) PEP treatment effectiveness: early PEP 100% and late PEP 100% effective (i.e., PEP effectiveness independent of infection-age); early PEP 100% and late PEP 50% effective; and early PEP 100% and late PEP 0% effective. We also studied a scenario considering PEP treatment effectiveness of 50% independent of infection-age. We did not study a scenario considering PEP treatment effectiveness of 0% independent of infection-age as it is similar to that where no PEP intervention is applied.

RIDT sensitivity and actual detection ratios

Interpreting sensitivity as a probability for detecting positives that is constant during infection justifies the assumption that a RIDT detection ratio is equal to the RIDT sensitivity value. However, just as the sensitivity of PCR diagnosis, the sensitivity of a RIDT may depend on the viral load of the tested individual, which varies during the infectious period. Indeed, studies show that RIDT performance is high when samples are collected one day after onset of symptoms and decreases progressively for samples which are collected later (Jernigan et al., 2011). RIDTs also seem to perform better with small children, who normally present a higher viral load than adults (Andresen and Kesson, 2010). Taking this into consideration we can hypothesise a time window when the RIDT performs better due to the patient having a high viral load. Consequently, if a majority of cases are sampled for diagnosis at a time when their viral load is peaking, even a rather insensitive RIDT may have a detection ratio larger than its reported sensitivity.

For our particular case of pandemic influenza in the Netherlands, Fig. 3 shows a viral load profile and the range of time that it remains above a hypothetical threshold for detection with a RIDT and with a PCR test. Estimating the RIDT sensitivity by randomly sampling patients at any infection-age would result in a value given by the ratio of 4.1 days (time window for positive RIDT) to 11.3 days (time window for positive PCR diagnosis), i.e., of about 36%. However, samples were collected according to the distribution shown in Fig. 3 (Table 1), meaning the detection ratio is given by the ratio of the dark-grey area to the total greyed area, i.e., about 60%. Following this procedure we evaluated the correlation between RIDT detection ratios and various RIDT sensitivities. Fig. 4 shows that the

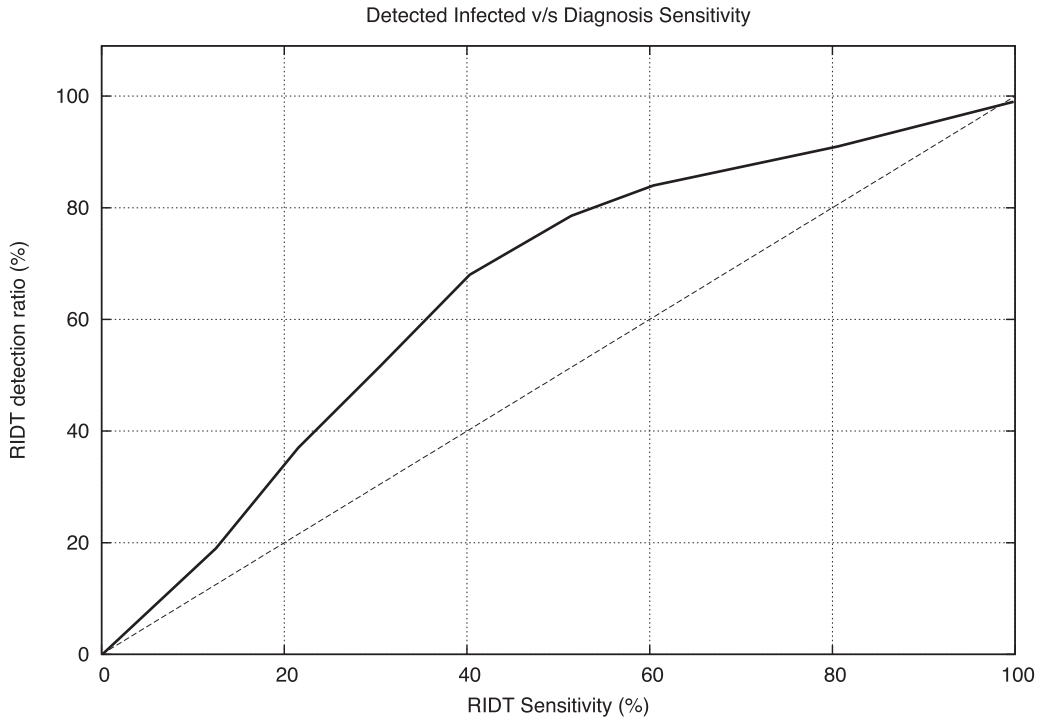

Fig. 4. Proportion of detected positives as a function of RIDT sensitivity. The solid line indicates the proportion of detected positives assuming the indicated RIDT test sensitivity, a time distribution for test sampling that matches the observed data and a time varying viral load as described in the text. The dotted line indicates a one to one relation.

detection ratio would be underestimated when considered equal to the sensitivity value, if cases are sampled near the viral load peak.

Knowing we can map RIDT detection ratios to RIDT sensitivities, we calculated and presented our results in terms of RIDT detection ratios. In this way they become more general and clear, as it is possible to later interpret results in terms of RIDT sensitivities, depending on any assumed correlation with RIDT detection ratios. The simplistic assumption that RIDT sensitivity is equivalent to the detection ratio provides the most conservative scenario.

Results

We performed 10,000 simulation runs of each model. Before considering the various R_0 values we studied, we focus in the models with a basic reproduction number $R_0 = 2$. This is value somewhat higher than that estimated for H1N1 (R_0=1.4–1.6, e.g., Fraser et al., 2009) but the effects we are studying are more clearly shown within a higher attack rate scenario (80% in a population where only cases after consultation are isolated and no PEP is provided to contacts). The attack rate values we present are the 95th-percentiles of the predicted outcomes for each modeled scenario (i.e., 95% of predicted attack rates are lower than the presented values). Fig. 5 shows final attack rates computed with scenarios assuming interventions based on bedside RIDTs with various detection ratios and PCR diagnostic tests, as indicated, and different PEP treatment effectiveness scenarios. RIDT based interventions perform better (have a lower attack rate) than PCR-diagnosis based interventions when the RIDT detection ratio is 100%, because PEP is provided earlier to all infected contacts. In contrast, when RIDT detection ratio is 0%, the attack rate is the same as not applying any kind of intervention to infected contacts (no PEP, solid thin line in Fig. 5), because no tested individual is detected positive.

An intervention based on the PCR diagnostic test has almost no effect if late PEP treatment is not effective (double-dotted lines in Fig. 5). Attack rates are almost the same as if no PEP treatment is administered to contacts because treatment is almost always applied after 48 h of infection (D_{CL}+D_{LX}+D_{XR} has a median of about 3 days). In this case, an intervention based on bedside RIDTs with any detection ratio larger than 0 performs better in reducing the final attack rate than the intervention based on the PCR diagnosis. Using bedside RIDT with 100% detection ratio would considerably reduce the attack rate to 25%, but still it would not be enough to avoid a large outbreak.

If late and early PEP treatments both have 100% effectiveness (dotted lines in Fig. 5), we see that a PCR-diagnosis based intervention reduces the attack rate considerably (to less than 30%). In order to achieve the same attack rate reduction with a bedside RIDT based intervention, the RIDT must have at least 60% detection ratio. A RIDT detection ratio of $\geq$70% would reduce the attack rate even further to the point of avoiding a large outbreak.

Considering the scenario with 100% effective early PEP treatment and 50% effective if applied after 48 h of infection (dashed lines in Fig. 5), the attack rate obtained with the PCR-diagnosis based intervention is 60%. Such an attack rate is matched by using a bedside RIDT-based intervention with 40% detection ratio. In this case the intervention is expected to avoid a large outbreak if the RIDT detection ratio is larger than 90%.

The scenario considering a constant PEP treatment effectiveness of 50% (tiny-dotted line in Fig. 5) exhibits for PCR diagnosis based interventions a very similar final attack rate as that of the mixed scenario with late PEP treatment effectiveness of 50%. The reason is that most PCR diagnosis based treatment is administered after 48 h, so there is little contribution from 100% effective early treatment. In contrast, interventions based on RIDTs perform significantly worse in this scenario than in the mixed scenario with 50% late PEP treatment effectiveness, as in this case there is an important proportion of treatments applied within 48 h of infection. Therefore, RIDTs need to have a detection ratio larger than 58% for a bedside RIDT based intervention to out perform a PCR diagnosis based intervention.

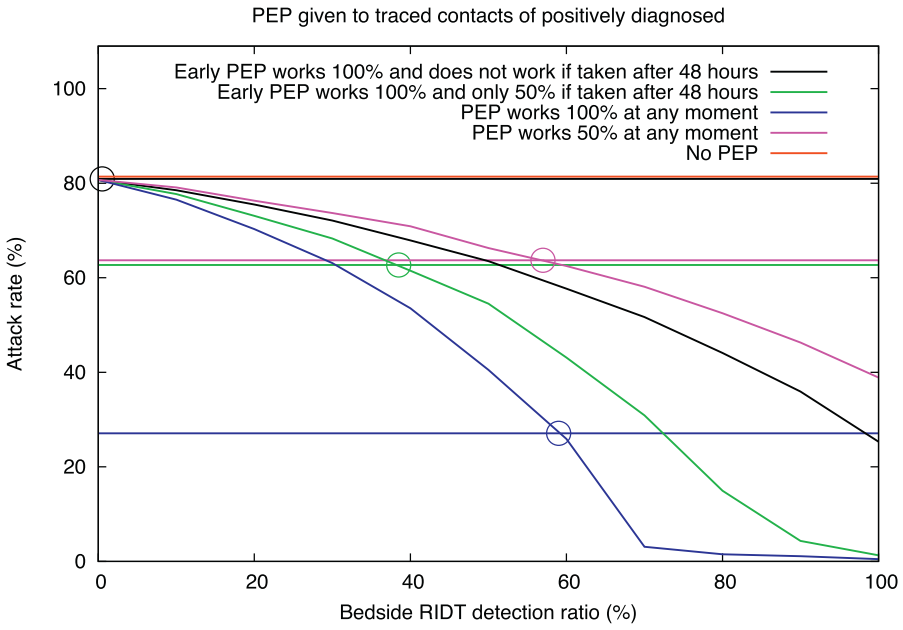

Fig. 5. Final attack rate of outbreaks ($R_0 = 2$) in which PEP treatment is provided to infected contacts, based on bedside RIDT with detection ratio indicated in the *x*-axis. Line colours show scenarios with different PEP treatment effectiveness, as indicated in the legend. Straight horizontal lines indicate the attack rate in case PCR-diagnosis based intervention is applied in the modelling scenario corresponding to their line styles. All lines show 95th-percentiles of the predicted outcomes of each indicated model in order to represent worst case scenarios. Circles highlight where RIDT-based interventions perform with the same efficacy as PCR-diagnosis based interventions for the corresponding scenario colour. (For interpretation of the references to color in this figure legend, the reader is referred to the web version of the article.)

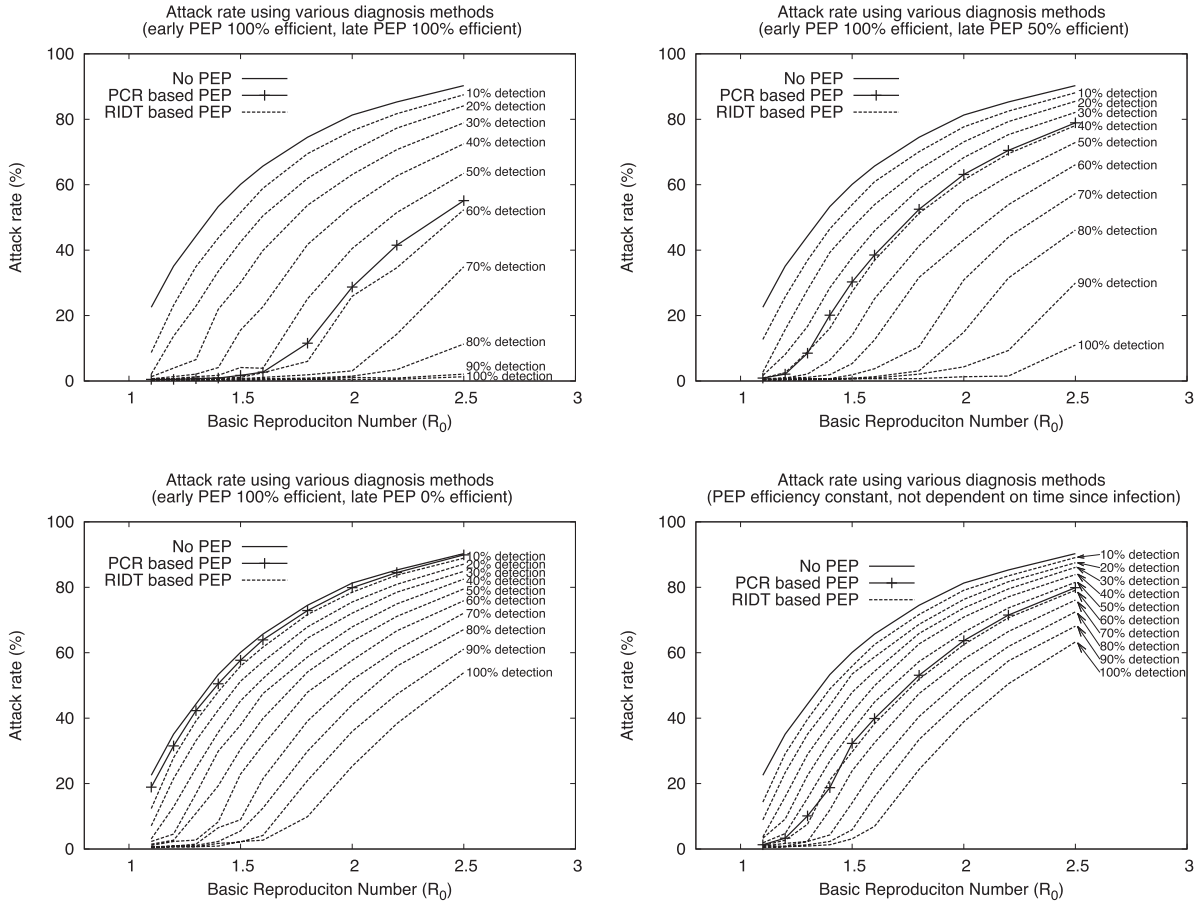

Fig. 6. Comparison of final attack rate as function of reproduction number considering interventions based on RIDTs performed at the bedside and interventions based on PCR-diagnosis (performed in the laboratory). Each panel indicates its corresponding scenario and efficiency of the PEP treatment provided to infected contacts. Each panel shows the indicated PEP treatment efficiency scenario. Bold solid lines indicate the predicted attack rates as if there is no treatment administered to contacts. Solid lines with crosses show the predicted attack rate of interventions based on PCR diagnostic tests. Dashed lines indicate predicted attack rates of RIDT based interventions, with RIDT detection ratios as indicated inside each panel.

Fig. 6 shows a similar analysis as above for varying R_0 values, from which those that are <2 lead to lower attack rates. While for the R_0 range of values estimated for H1N1 (1.4–1.6) PCR-diagnosis based interventions have outbreak control potential only when PEP treatment is 100% effective at any time of administration, bedside RIDT based interventions are potentially capable of outbreak control in all considered scenarios of treatment effectiveness, depending on the detection ratio of RIDTs. Lines showing attack rate do no cross in Fig. 6, indicating that varying R_0 does not change which intervention performs better than another. Therefore, the predicted minimum detection ratio a RIDT should have for an intervention based on it to perform equally as well as one based on PCR diagnosis is independent of R_0, for a given PEP treatment effectiveness. This is also visualised in Fig. 7, which shows $R_{\mathcal{I}}$ as a function of R_0 for various interventions. For each intervention there is a linear relation showing the reduction factor of the reproduction number is independent of R_0, except for when $R_{\mathcal{I}}$ and R_0 approximately equal 1, which is the threshold limit for outbreaks to occur.

Fig. 8 shows the comparison between scenarios with interventions based on RIDTs performed at laboratory facilities and with interventions based on PCR diagnostics. Similar qualitative conclusions are drawn as in the previous comparison where bedside RIDTs are considered, but attack rate differences are smaller because infected contacts are provided PEP treatment with a larger delay than in the scenarios when RIDTs are performed at the bedside. For the same reason, larger laboratory-RIDT detection ratios than those for bedside RIDTs are needed to match interventions based on PCR tests.

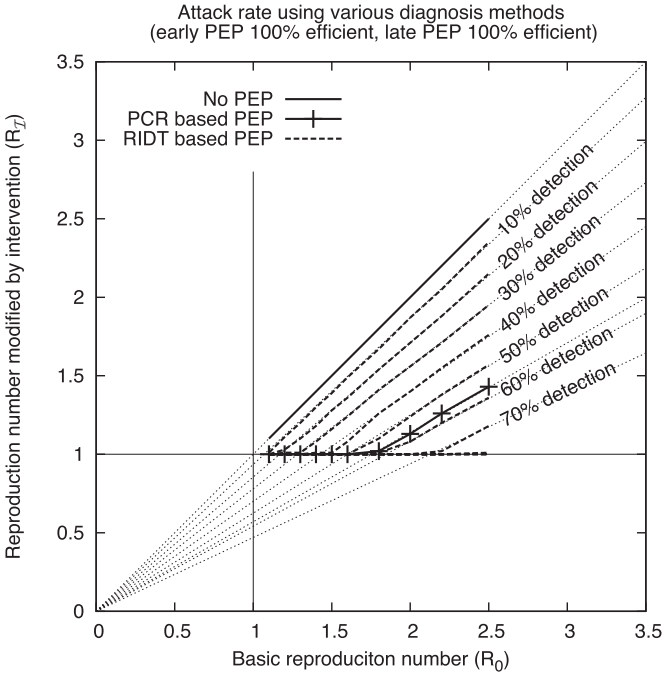

Fig. 7. Reproduction number modified by PEP intervention on contacts compared to reproduction number of baseline scenario (no PEP given to contacts). The bold solid line indicate $R_{\mathcal{I}} = R_0$ when there is no treatment administered to contacts. Solid line with crosses show predicted $R_{\mathcal{I}}$ (approximately $0.57R_0$) for interventions based on PCR diagnostic tests. Dashed lines indicate predicted $R_{\mathcal{I}}$ for RIDT based interventions, with RIDT detection ratios as indicated in the figure. Thin dotted diagonal lines are for showing the linearity of the relation between $R_{\mathcal{I}}$ and R_0.

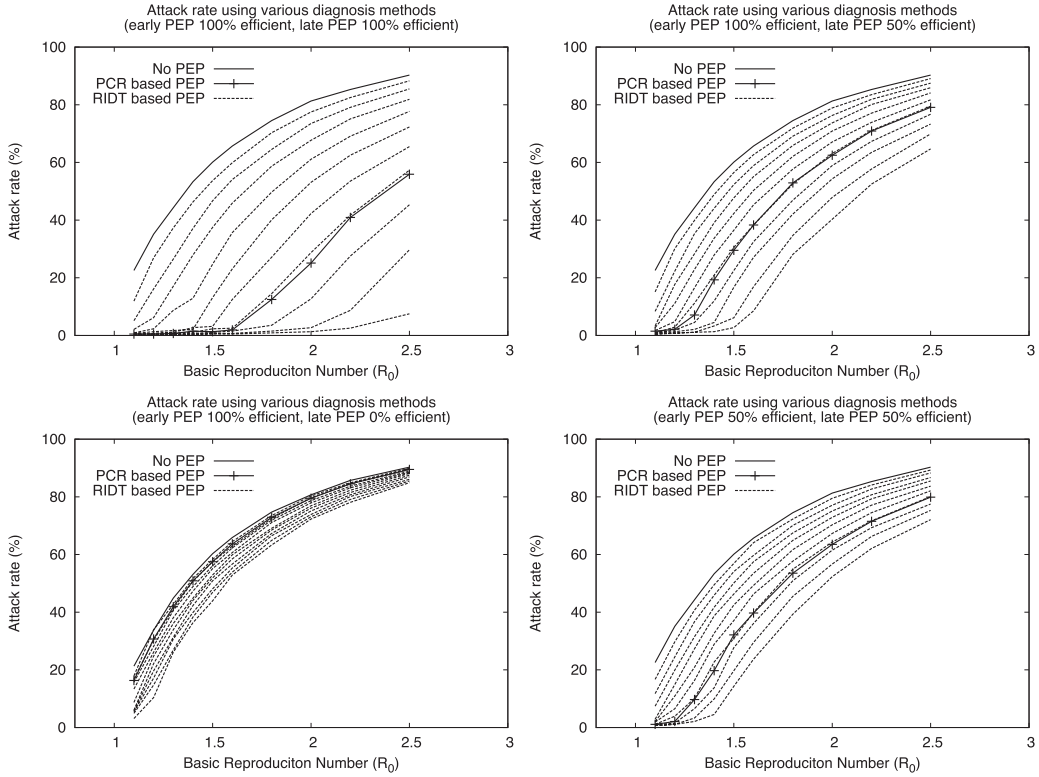

Fig. 8. Comparison of final attack rate as function of reproduction number considering interventions based on RIDTs performed in the laboratory and on PCR-diagnosis (also performed in the laboratory). Bold solid lines indicate the predicted attack rates as if there is no treatment administered to contacts. Solid lines with crosses show the predicted attack rate of interventions based on PCR diagnostic tests. Dashed lines indicate predicted attack rates of RIDT based interventions, with RIDT detection ratios varying from 10% (higher attack rates) to 100% (lower attack rates), increasing in steps of 10%. These are respectively presented from higher to lower attack rates for any given reproduction number value, in the same way as in Fig. 6.

Discussion

We showed that using RIDTs in place of PCR-diagnosis potentially leads to an equally or more effective intervention even with lower sensitivities, depending on the effectiveness of PEP treatment. The most favourable situation for a PCR-diagnosis based intervention is the case that PEP treatment is 100% effective, regardless of when it is administered. In this situation, we find that employing a bedside RIDT based intervention requires a $\geq$60% detection ratio and a laboratory RIDT based intervention a $\geq$70% detection ratio for achieving the same results. These results do not only manifest in the final attack rates, but also in the attack rates at any moment during the outbreak (see Appendix A). In a more realistic scenario where PEP treatment is less effective if applied later, even lower RIDT detection ratios are sufficient to match performance of a PCR based intervention. A 60% detection ratio is already within the range measured for existing RIDTs [e.g., Balish et al., 2009, Jernigan et al., 2011]. Therefore our analysis suggests that for the 2009 H1N1 outbreak, the use of an existing RIDT at the moment of sample collection would have been preferable over using PCR diagnostic tests for implementing interventions.

Besides attack rates, there are other ways for comparing the performance of interventions which may be more directly applicable from a logistic point of view, such as reduction of number of people in the contact tracing system, reduction of number of people needing treatment, and reduction of (peak) incidence. However, provided that a particular intervention when compared to another keeps the prevalence lower at any given moment during the outbreak, we expect that everything that scales in a per-case manner is also kept at lower numbers.

Our results show that given two particular interventions, the one leading to a lower attack rate does so for all R_0 value in the range we considered, except for when R_0 is so small that both interventions can achieve outbreak control. Moreover, we show that any particular intervention reduces the reproduction number by a factor which does not depend on R_0. This indicates that the trade off between speed and coverage does not depend on the magnitude (i.e., R_0) but rather on the shape of the average individual reproduction density ($\varrho(\tau)$) and of the infection-age distribution of intervention implementation. The distribution in time of intervention implementation on contacts depends on when during the infection diagnostic samples are collected and on the duration of the various delays until having a diagnostic test result. Information on those variables can be directly collected. Observing the shape of the individual reproduction density is more difficult as generation interval distributions are required (Wallinga and Lipsitch, 2007). Generation intervals indicate the time between infection of the primary case to infection of secondary cases and their distributions are difficult to observe directly. However, observing serial interval distributions (time between symptom onset of primary case to symptom onset of secondary cases) is possible and these can be used to estimate generation intervals and, therefore, the distribution of the individual reproduction density [e.g., Klinkenberg and Nishiura, 2011].

Considering that RIDT sensitivity depends on the viral load of the tested subject at the moment of sampling, the proportion of detected cases may vary and differ from the measured sensitivity. If testing takes place during infectious stages with high viral load, the 60% bedside RIDT detection ratio necessary for matching the performance of a PCR-diagnosis based intervention could be achieved already with a test of less than 40% sensitivity. For a laboratory RIDT (70%) the same holds for less than 50% sensitivity (Fig. 4). This suggests that had we used RIDTs existing at the time of onset of the novel influenza A (H1N1) epidemic as diagnostic tests the impact of prophylactic treatment of contacts would have been equal or even higher than when using PCR tests. In addition, high viral load levels are associated with higher infectivity. Thus, testing at the moment of higher viral loads not only increases the probability of getting a positive result but also intervening when they have a higher transmission potential, thereby making RIDT-based interventions even more effective.

In our analysis we assume an intervention with 100% coverage, so neither under-reporting, non-compliance, missing contacts, nor the possibility of asymptomatic cases are considered. In case the intervention coverage is not 100%, both RIDT and PCR-diagnosis based interventions are less effective in reducing attack rates of an epidemic as both would be applied only to a fraction of the infected population. Our findings on which intervention would perform better than the other remain valid for that subpopulation and therefore generalise to the total population, but with smaller differences in performance (e.g., Appendix B).

Our analysis includes individual heterogeneity in R_j and $R_{\mathcal{I},j}$, as a consequence of the stochasticity in the duration of the various delays in the transmission and intervention time-lines. However, we have not carried out simulations including more than random heterogeneity, such as super-spreading events. The later can play a significant role in the early stages of an outbreak (Lloyd-Smith et al., 2005), which is when case-based interventions are likely to be implemented. For example, super-spreading events could render interventions based on low sensitivity diagnosis tests less effective, as the possibility of missing these events (which are few) is increased.

It has been proposed that interventions including anti-viral treatment may promote the emergence of a drug resistant virus strain due to selective pressure exerted by the number of people treated with anti-viral drugs (Lipsitch et al., 2007). Considering this into our analysis would favour the decision of using RIDT-based interventions as these can be equally as effective as PCR-based interventions while fewer people receive anti-viral treatment.

Conclusion

The concept of individual reproduction density proved useful for analysing the impact of interventions targeted at high risk individuals during epidemic outbreaks when a trade off between speed and coverage is at play. We find that using a bedside RIDT with 60% detection ratio or a laboratory RIDT with 70% detection ratio is already sufficient to match the performance of the best PCR-diagnosis based interventions. Even lower RIDT detection ratios are sufficient to match the performance of PCR-diagnosis based interventions if post exposure prophylaxis is not 100% effective. Employing the method described here provides insight in relative impact of interventions. In combination with data collected during outbreaks such as serial intervals and viral load distributions the results may be applied to support policy making decisions in the future.

Appendix A. Attack rates comparison at different time points during the outbreak

In the interest of public health authorities, we present our results on how the various modelled interventions based on bedside RIDTs would help slowing down ongoing outbreaks, and how they compare to PCR-based interventions. Figs. A.9–A.13 show attack rate comparisons as observed respectively at 30, 60, 90, 120 and 180 days after the beginning of the outbreak, for the same R_0 values considered in Fig. 6. Whether any intervention performs better than another appear independent of R_0 in each figure, in a similar way as in Fig. 6. Only in Fig. A.9 results for a better performing intervention do not consistently remain better for different values of R_0 because of enhancement of stochastic effects due to smaller

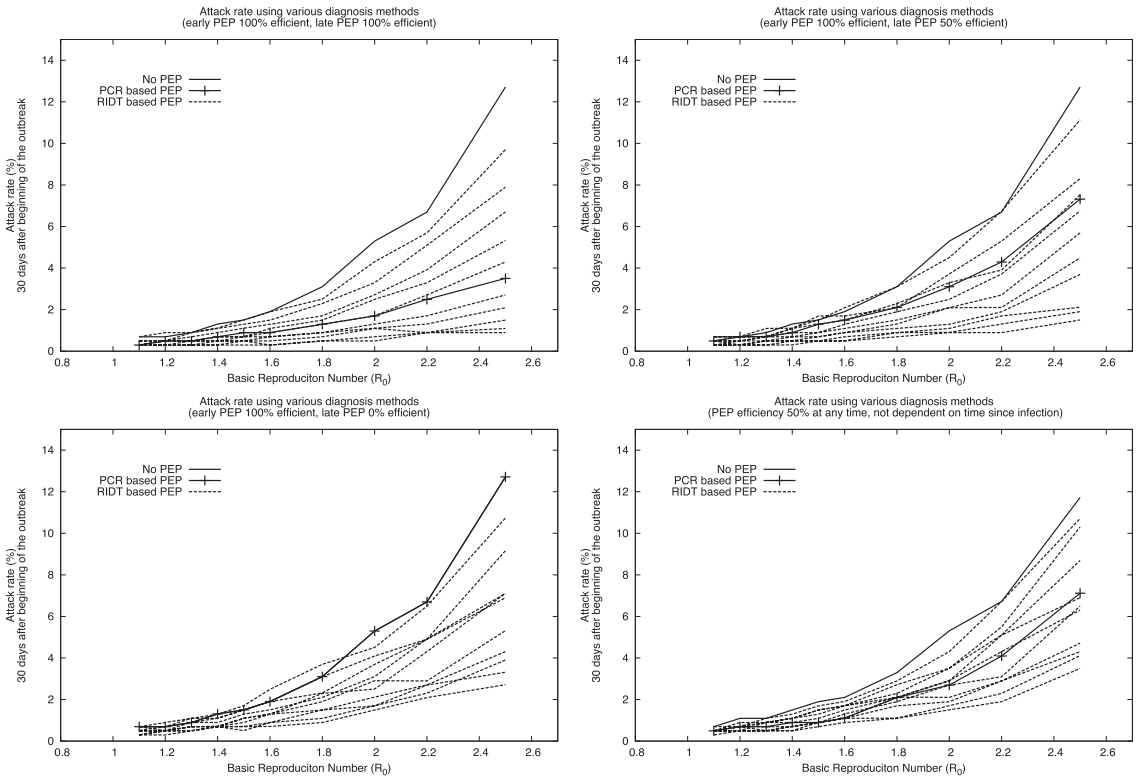

Fig. A.9. Attack rate observed 30 days after outbreak has begun as function of reproduction number. Each panel indicates its corresponding scenario and efficiency of the PEP treatment provided to infected contacts. Bold solid lines indicate the predicted attack rates as if there is no treatment administered to contacts. Solid lines with crosses show the predicted attack rate of interventions based on PCR diagnostic tests. Dashed lines indicate predicted attack rates of bedside RIDT based interventions, with RIDT detection ratios varying from 10% (higher attack rates) to 100% (lower attack rates), increasing in steps of 10%. These are respectively presented from higher to lower attack rates for any given reproduction number value, in the same way as in Fig. 6.

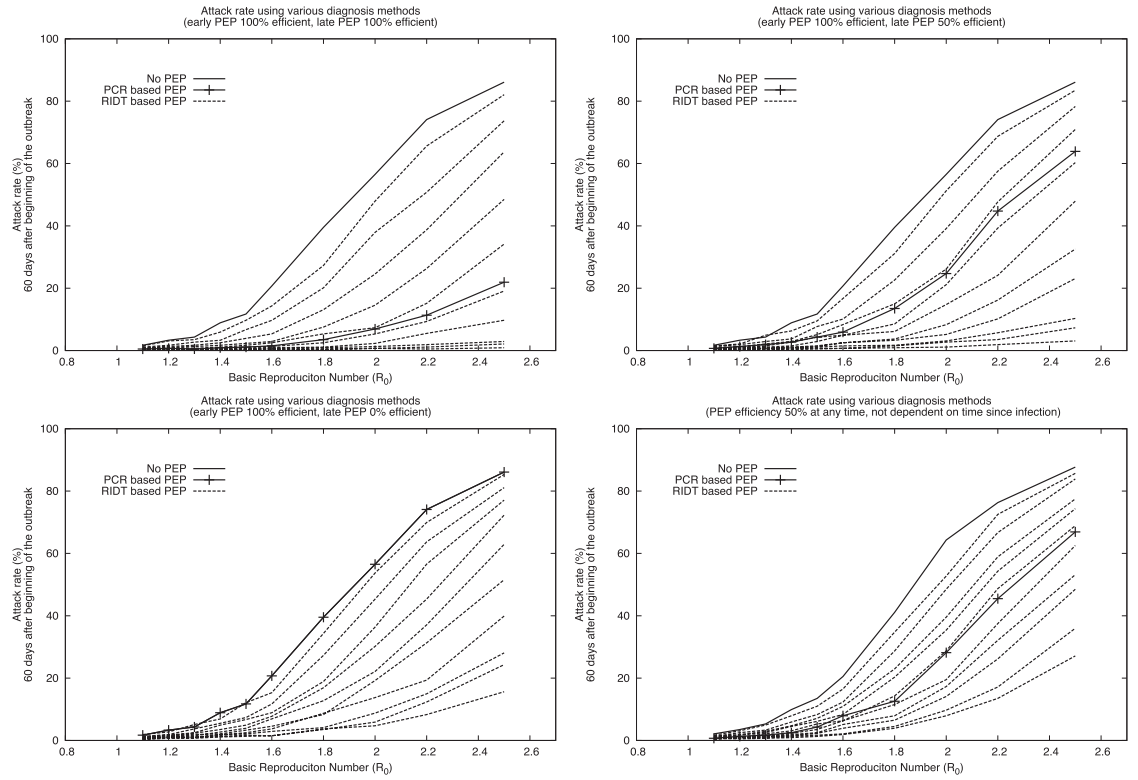

Fig. A.10. Similar to Fig. A.9, but with attack rates observed 60 days after outbreaks have begun.

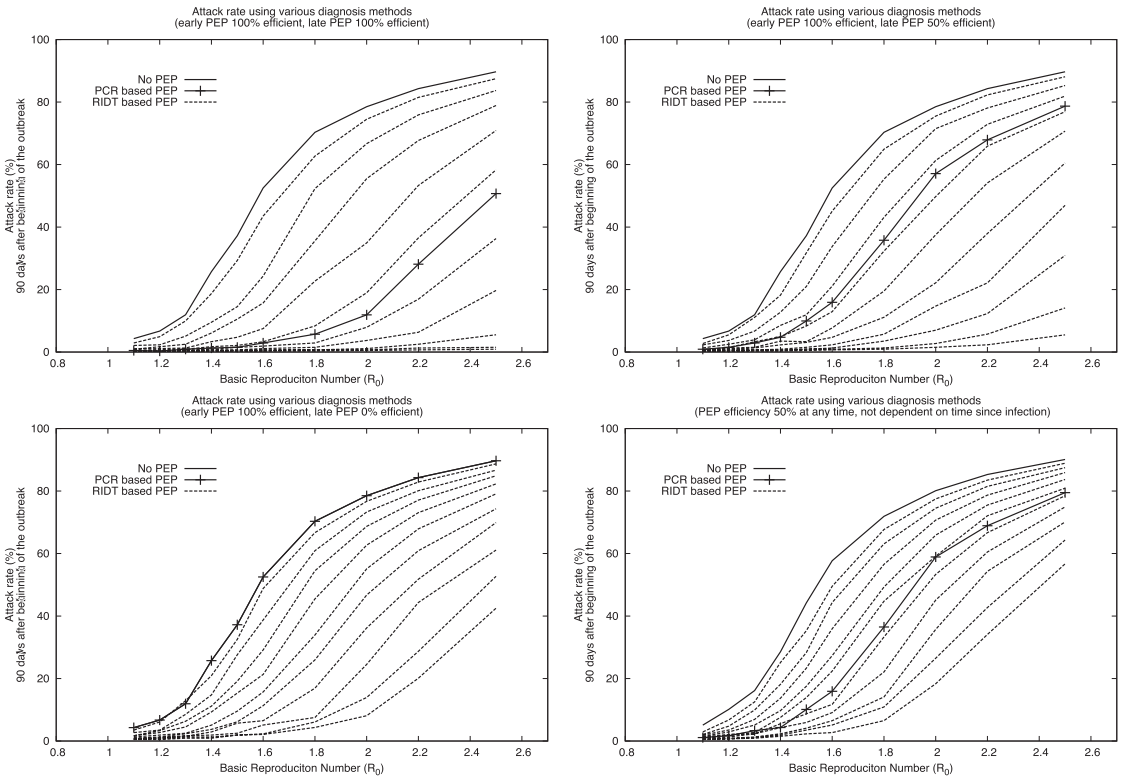

Fig. A.11. Similar to Fig. A.9, but with attack rates observed 90 days after outbreaks have begun.

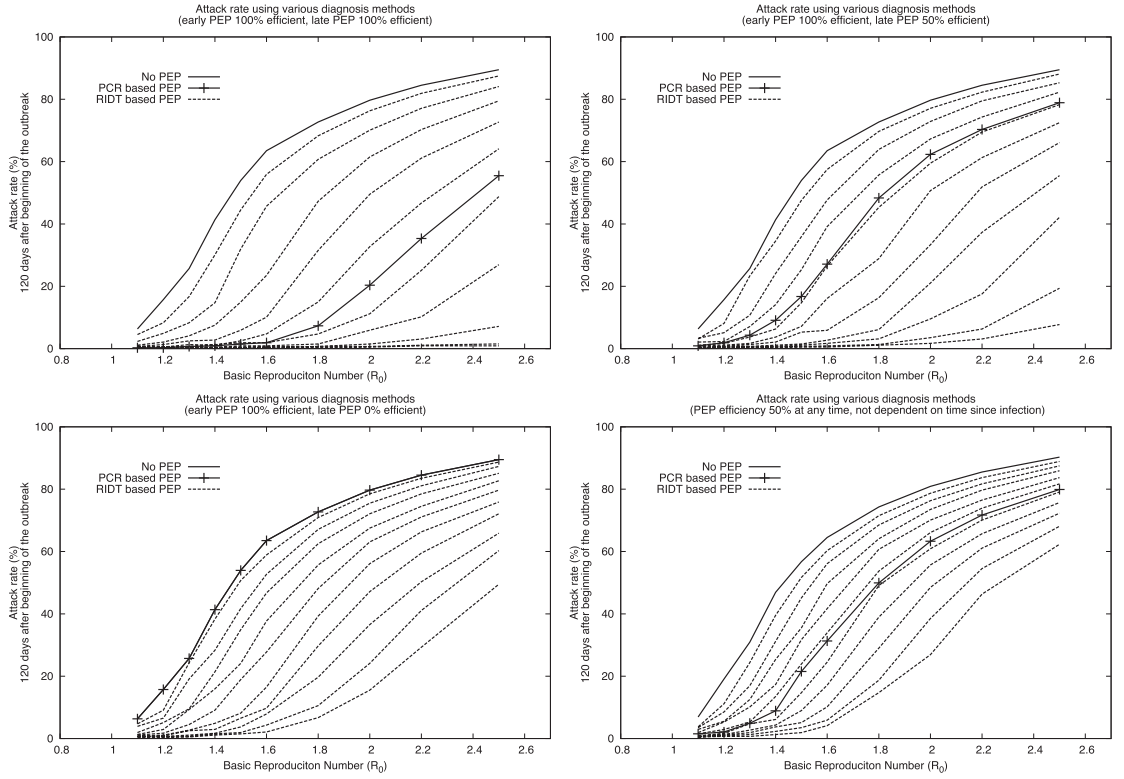

Fig. A.12. Similar to Fig. A.9, but with attack rates observed 120 days after outbreaks have begun.

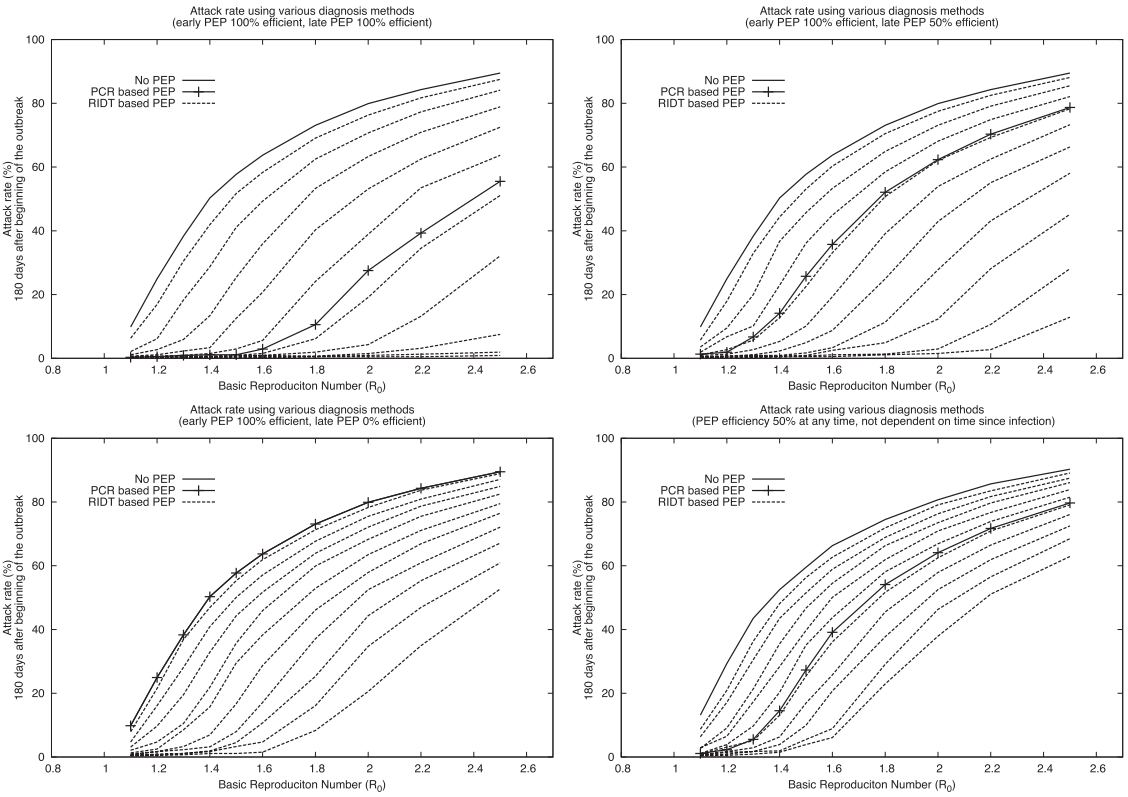

Fig. A.13. Similar to Fig. A.9, but with attack rates observed 180 days after outbreaks have begun.

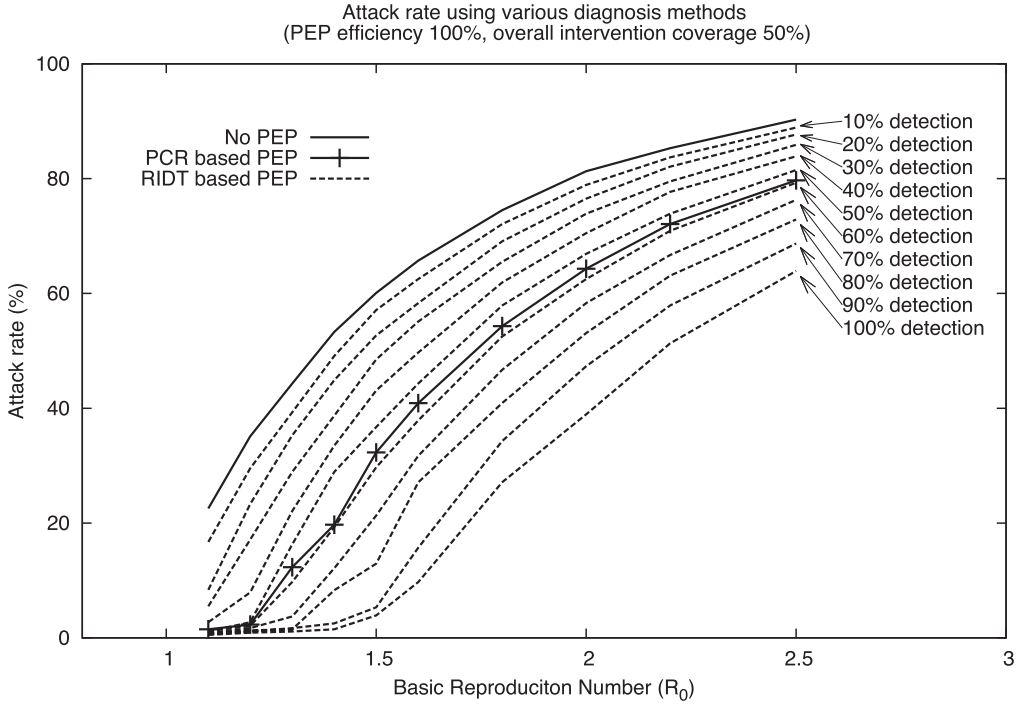

Fig. B.14. Comparison of final attack rate as function of reproduction number considering interventions based on RIDTs performed at the bedside and interventions based on PCR-diagnosis (performed in the laboratory). Bold solid lines indicate the predicted attack rates as if there is no treatment administered to contacts. Solid lines with crosses show the predicted attack rate of interventions based on PCR diagnostic tests. Dashed lines indicate predicted attack rates of RIDT based interventions, with RIDT detection ratios as indicated inside each panel.

numbers. In general, any intervention that has a better performance reducing the outbreak final size will also perform better by further reducing the number of infections at any point in time during the outbreak.

Appendix B. Attack rates comparison assuming lower overall coverage

In practice, conditions are far from ideal to implement case-based interventions with high coverage. Overall coverage of any intervention is reduced by many factors such as the sensitivity of the gold standard diagnostic method, impossibility of tracing of all possible contacts, non-compliance to take antiviral drugs, under-reporting, among others. All these factors will add up in a multiplicative mannerto reduce the proportion of the population which can be reached by a contact-based intervention. Here we present our results by assuming that the contact-based intervention is applied on 50% of the population, assuming that PEP efficiency is 100% independent of the infection-age at which prophylaxis is administered. The attack rate of all interventions is larger in comparison to the case considering 100% overall intervention coverage in the manuscript (except for the case when there is no PEP administered). However, when comparing interventions among each other we see that an intervention based on a bedside RIDT with 60% sensitivity has a performance comparable to an intervention based on PCR-diagnosis, just as in the case considering 100% overall intervention coverage. This is expected because RIDT sensitivities are measured relative to the PCR method. Therefore, the coverage of both RIDT and PCR based interventions are reduced in the same proportion, maintaining their relative performance regarding which of the interventions leads to lower attack rate.

Fig. B.14.

References

Anderson, R.M., May, R.M., 1991. Infectious Diseases of Humans. Dynamics and Control. Oxford University Press.

Andresen, D.N., Kesson, A.M., 2010. High sensitivity of a rapid immunochromatographic test for detection of influenza A virus 2009 H1N1 in nasopharyngeal aspirates from young children. J. Clin. Microbiol. 48 (July), 2658–2659.

Balish, A., Warnes, C., Wu, K., Barnes, N., Emery, S., Berman, L., Shu, B., Lindstrom, S., Xu, X., Uyeki, T., Shaw, M., Klimov, A., Villanueva, J., 2009. Influenza div, national center for immunization and respiratory diseases, CDC. Evaluation of rapid influenza diagnostic tests for detection of novel influenza A (H1N1) Virus – United States, 2009. MMWR Morb. Mortal. Wkly. Rep. 58 (August), 826–829.

Bonačić Marinović, A.A., Swaan, C., Wichmann, O., van Steenbergen, J., Kretzschmar, M., 2012. Effectiveness and timing of vaccination during school measles outbreak. Emerg. Infect. Dis. 18 (September (9)), 1405–1413.

Bouscambert Duchamp, M., Casalegno, J.S., Gillet, Y., Frobert, E., Bernard, E., Escuret, V., Billaud, G., Valette, M., Javouhey, E., Lina, B., Floret, D., Morfin, F., 2010. Pandemic A(H1N1)2009 influenza virus detection by real time RT-PCR: is viral quantification useful? Clin. Microbiol. Infect. 16 (April (4)), 317–321.

Carrat, F., Vergu, E., Ferguson, N.M., Lemaitre, M., Cauchemez, S., Leach, S., Valleron, A.J., 2008. Time lines of infection and disease in human influenza: a review of volunteer challenge studies. Am. J. Epidemiol. 167 (April (7)), 775–785.

CDC, 2009, December. CDC H1N1 Flu – Updated Interim Recommendations for the Use of Antiviral Medications in the Treatment and Prevention of Influenza for the 2009–2010 Season. http://www.cdc.gov/h1n1flu/recommendations.htm

Cori, A., Valleron, A.J., Carrat, F., Scalia Tomba, G., Thomas, G., Boelle, P.Y., 2012. Estimating influenza latency and infectious period durations using viral excretion data. Epidemics 4 (August (3)), 132–138.

Crawford, J.M., Stallone, R., Zhang, F., Gerolimatos, M., Korologos, D.D., Sweetapple, C., de Geronimo, M., Dlugacz, Y., Armellino, D.M., Ginocchio, C.C., 2010 Jan. Laboratory surge response to pandemic (H1N1) 2009 outbreak, New York City metropolitan area, USA. Emerg. Infect. Dis. 16 (1), 8–13.

Diekmann, O., Heesterbeek, J., Britton, T., 2012. Mathematical Tools for Understanding Infectious Disease Dynamics. Princeton University Press.

Dolin, R., 1976. Influenza: current concepts. Am. Fam. Phys. 14 (September), 72–77.

Fraser, C., Donnelly, C.A., Cauchemez, S., Hanage, W.P., Van Kerkhove, M.D., Hollingsworth, T.D., Griffin, J., Baggaley, R.F., Jenkins, H.E., Lyons, E.J., Jombart, T., Hinsley, W.R., Grassly, N.C., Balloux, F., Ghani, A.C., Ferguson, N.M., Rambaut, A., Pybus, O.G., Lopez-Gatell, H., Alpuche-Aranda, C.M., Chapela, I.B., Zavala, E.P., Guevara, D.M.E., Checchi, F., Garcia, E., Hugonnet, S., Roth, C., 2009. Pandemic potential of a strain of influenza a (H1N1): early findings. Science 324 (June (5934)), 1557–1561, PMID:19433588.

Hahné, S., Donker, T., Meijer, A., Timen, A., van Steenbergen, J., Osterhaus, A., van der Sande, M., Koopmans, M., Wallinga, J., Coutinho, R., 2009. Epidemiology and control of influenza a(H1N1)v in the Netherlands: the first 115 cases. Euro Surveill. 14 (July (27)), PMID:19589332.

Heymann, D.L. (Ed.), 2008. Control of Communicable Diseases Manual. , 19th ed. American Public Health Association.

Jernigan, D.B., Lindstrom, S.L., Johnson, J.R., Miller, J.D., Hoelscher, M., Humes, R., Shively, R., Brammer, L., Burke, S.A., Villanueva, J.M., Balish, A., Uyeki, T., Mustaquim, D., Bishop, A., Handsfield, J.H., Astles, R., Xu, X., Klimov, A.I., Cox, N.J., Shaw, M.W., 2011. Detecting 2009 pandemic influenza A (H1N1) virus infection: availability of diagnostic testing led to rapid pandemic response. Clin. Infect. Dis. 52 (January (Suppl. 1)), 36–43.

Klinkenberg, D., Nishiura, H., 2011. The correlation between infectivity and incubation period of measles, estimated from households with two cases. J. Theor. Biol. 284 (September), 52–60.

Lipsitch, M., Cohen, T., Murray, M., Levin, B.R., 2007. Antiviral resistance and the control of pandemic influenza. PLoS Med. 4 (January (1)), e15.

Lloyd-Smith, J., Schreiber, S., Kopp, P., Getz, W., 2005. Superspreading and the effect of individual variation on disease emergence. Nature 438, 355–359.

Meijer, A., Beerens, A., Claas, E., Hermans, M., de Jong, A., Molenkamp, R., Niesters, H., Overduin, P., Rossen, J., Schuurman, R., Wolffs, P., Fouchier, R., Osterhaus, A., Schutten, M., Koopmans, M., 2009. Preparing the outbreak assistance laboratory network in the Netherlands for the detection of the influenza virus a(H1N1) variant. J. Clin. Virol. 45 (July (3)), 179–184, PMID:19540155.

Richardson, M., Elliman, D., Maguire, H., Simpson, J., Nicoll, A., 2001. Evidence base of incubation periods, periods of infectiousness and exclusion policies for the control of communicable diseases in schools and preschools. Pediatr. Infect. Dis. J. 20, 380–391.

RIVM, 2010. Guidelines for Infectious Diseases, 2010. Rijksinstituut voor Volksgezondheid en Milieu (RIVM – National Institute for Public Health and the Environment), Centrum Infectieziektebestrijding (CIb – Center for Infectious Disease Control), The Netherlands. http://www.rivm.nl/cib/infectieziekten-A-Z/infectieziekten/

van Asten, L., van der Lubben, M., van den Wijngaard, C., van Pelt, W., Verheij, R., Jacobi, A., Overduin, P., Meijer, A., Luijt, D., Claas, E., Hermans, M., Melchers, W., Rossen, J., Schuurman, R., Wolffs, P., Boucher, C., Bouchier, C., Schirm, J., Kroes, L., Leenders, S., Galama, J., Peeters, M., van Loon, A., Stobberingh, E., Schutten, M., Koopmans, M., 2009. Strengthening the diagnostic capacity to detect bio safety level 3 organisms in unusual respiratory viral outbreaks. J. Clin. Virol. 45 (July (3)), 185–190, PMID:19515608.

van Boven, M., Donker, T., van der Lubben, M., van Gageldonk-Lafeber, R.B., te Beest, D.E., Koopmans, M., Meijer, A., Timen, A., Swaan, C., Dalhuijsen, A., Hahne, S., van den Hoek, A., Teunis, P., van der Sande, M.A., Wallinga, J., 2010. Transmission of novel influenza A(H1N1) in households with post-exposure antiviral prophylaxis. PLoS ONE 5 (7), e11442.

Vinikoor, M., Stevens, J., Nawrocki, J., Singh, K., 2009. Influenza a virus subtyping: paradigm shift in influenza diagnosis. J. Clin. Microbiol. 47 (9), 3055–3056, http://dx.doi.org/10.1128/JCM.01388-09.

Wallinga, J., Lipsitch, M., 2007. How generation intervals shape the relationship between growth rates and reproductive numbers. Proc. Biol. Sci. 274 (February), 599–604.